



## Microplastics in a salt-wedge estuary: Vertical structure and tidal dynamics

Sophie Defontaine<sup>a</sup>, Damien Sous<sup>b,c,\*</sup>, Javier Tesan<sup>b</sup>, Mathilde Monperrus<sup>d</sup>, Véronique Lenoble<sup>b</sup>, Laurent Lanceleur<sup>d</sup>



<sup>a</sup> CNRS/Univ. Pau & Pays Adour/E2S UPPA, Laboratoire de Mathématiques et de leurs Applications de Pau - Fédération MIRA, UMR5142, 64000 Pau, France

<sup>b</sup> Université de Toulon, Aix Marseille Université, CNRS, IRD, Mediterranean Institute of Oceanography (MIO), La Garde, France

<sup>c</sup> Univ. Pau & Pays Adour/E2S UPPA, Laboratoire des Sciences de l'Ingénieur Appliquées à la Mécanique et au Génie Électrique (SIAME) - MIRA, EA4581, 64600 Anglet, France

<sup>d</sup> Université de Pau et des Pays de l'Adour, E2S UPPA, CNRS, IPREM, Anglet, France

### ARTICLE INFO

**Keywords:**  
Salt-wedge estuary  
Microplastics  
Vertical distribution  
Field sampling  
Numerical Modelling

### ABSTRACT

The abundance and distribution of microplastics in estuaries have been barely documented, and generally without accounting for the vertical structure in the water column. This study presents the very first data on the occurrence and distribution of microplastics in the Adour Estuary, SW France. The experimental data set was complemented by numerical simulations to gain understanding of the behaviour of suspended microplastics. Microplastics were found throughout the water column with a mean abundance of 1.13 part/m<sup>3</sup>. Films and fragments were the most abundant types of particles collected. Numerical simulations demonstrated that vertical distribution of microplastics in the water column is highly dependent on particle characteristics and on the local hydrodynamics. The main trend is that neutrally-buoyant microplastics are easily flushed out while heavier microplastics are prone to entrapment in the estuary, in particular under low discharge conditions. The present study suggest that estuaries could be a sink of microplastics.

### 1. Introduction

Microplastics, commonly defined as plastics with the largest dimension below 5 mm (Collignon et al., 2014), are now readily recognized as ubiquitous in the environment. They can be directly produced for industrial use (i.e. primary source) or they can be generated by mechanical, photochemical and/or biological degradation of larger plastic debris (i.e. secondary source). Most of the microplastics found in oceans derives from land-based larger plastic litter (Andrady, 2011). A series of recent reviews has described the growing threat of plastics pollution for marine ecosystems (Barboza and Gimenez, 2015; do Sul and Costa, 2014; Law, 2017; Rezania et al., 2018; Xanthos and Walker, 2017). Microplastics, by their similar dimension to sediments and planktonic organisms, can easily be mistaken for food and ingested by marine biota (Browne et al., 2008; Lima et al., 2014). Potential impacts of ingestion of microplastics are various, such as gut blockage, abrasion of the digestive system, reduced growth rates and reproductive deficiency (Galgani et al., 2010; Wright et al., 2013). In addition, microplastics can adsorb contaminants such as persistent organics and metals contained in the water (Bakir et al., 2014; Brennecke et al., 2016; Yonkos et al., 2014). Thus, organisms ingesting microplastics may assimilate sorbed contaminants, as well as toxic additives used in the

compounding of plastics and bacteria encrusted on microplastics, leading to additional threats (Andrady, 2011). The ubiquity and abundance of microplastics increase the risks for marine and estuarine ecosystems. Lima et al. (2014) showed that in the Goiana Estuary (Brasil) the quantity of microplastics in the water column can surpass the abundance of planktonic fish eggs and larvae.

Microplastics have been found in nearly every compartment of nearshore and open ocean systems, including in the water column, sediments or living organisms (Crawford and Quinn, 2017; Cressey, 2016; Thompson et al., 2004; van Sebille et al., 2012). Nearly 96% of the global amount of ocean microplastics originate in continents, i.e. mainly convected by rivers (Boucher and Friot, 2017; Browne et al., 2011). Recently Lebreton et al. (2017) estimated that between 1.15 and 2.41 million tons of plastic waste enter ocean every year through rivers. By their location at the interface between ocean and rivers, estuaries are of outstanding importance to gain knowledge on the dispersion mechanisms of microplastics. As estuaries are densely populated and industrialized, they represent an additional source of microplastics contamination. Understanding the behaviour of plastics in estuarine environments is not simple and involves a range of processes which are not yet fully understood despite the growing number of dedicated studies. A common observation is that estuaries worldwide face

\* Corresponding author at: Université de Toulon, Aix Marseille Université, CNRS, IRD, Mediterranean Institute of Oceanography (MIO), La Garde, France.  
E-mail address: [sous@univ-tln.fr](mailto:sous@univ-tln.fr) (D. Sous).

microplastics contamination and have been identified as microplastics hotspots (Fok and Cheung, 2015; Simon-Sánchez et al., 2019). Experimental studies have been carried out in each aquatic compartment: biota (Abbas et al., 2018; Browne et al., 2008; Li et al., 2018), water (Gallagher et al., 2016; Gray et al., 2018; Lima et al., 2015; Sadri and Thompson, 2014; Xu et al., 2018; Yan et al., 2019; Yonkos et al., 2014; Zhao et al., 2015) and sediment (Gray et al., 2018; Naidoo et al., 2015; Peng et al., 2017; Simon-Sánchez et al., 2019; Willis et al., 2017).

For the water compartment, experimental and numerical approaches are generally limited to floating microplastics, such as surface sampling and 2D Lagrangian particle-tracking models coupled with ocean circulation models (Isobe et al., 2009; Kako et al., 2010; Lebreton et al., 2012; Murray et al., 2018; Neumann et al., 2014; Sherman and Van Sebille, 2016), assuming that most of the microplastics load is floating (Mani et al., 2015; McCormick et al., 2016; Yonkos et al., 2014), and focusing on the longitudinal spread of the plastics load from cities and sewage plants (Dris et al., 2018; Mani et al., 2015). The floating-particle assumption is probably partly valid at large scale in the open ocean where most heavy particles would have sunk well beyond the resuspension (closure) depth. However, the vertical structure of the plastics load can certainly not be ignored in coastal and estuarine environments where the hydrodynamics is generally able to maintain in suspension sediments which are heavier than typical polymers (Forsberg et al., 2020; Jalón-Rojas et al., 2019; Kukulka et al., 2012). To numerically study the dispersion of microplastics in areas of intense turbulence or wave mixing, it was shown that vertical turbulence model and particle inertia are key parameters (DiBenedetto et al., 2018; Jalón-Rojas et al., 2019; Stocchino et al., 2019). The vertical structure of the microplastics load remains very poorly documented in the field, in particular in the presence of strong vertical variations of density and turbulent mixing such as observed in salt-wedge estuaries. While a growing research effort has been engaged to estimate the occurrence, distribution and composition of surface microplastics, no study has investigated the presence and abundance of microplastics along the vertical plane in estuarine systems. This issue is of particular importance in the challenging context of salt-wedge estuaries, where the competition between density stratification and turbulent mixing can drastically affect the behaviour of water masses and suspended particles. In the Adour Estuary, intense periods of mixing (i.e. ebb) followed by strong stratification periods (i.e. flood) have a great impact on the behaviour of suspended sediment (Defontaine et al., 2019). Similarly, microplastic distributions is expected to be strongly affected by the complex estuarine hydrodynamics, impacting the contamination of both inner estuary and connected coastal waters.

In addition, from a methodological point of view, the estuarine environment makes field sampling very difficult due to the variable bathymetry, intense currents and harbor activities. Commonly used sampling methods may be difficult to deploy in this environment. For instance small trawl nets (e.g. "Manta" nets), commonly used for surface water sampling, are generally towed at the rear of boats at a speed below 3 knots which is comparable or even lower than the surface ebbing velocities reached in a lot of estuaries. The repetition of trawling operations can also be greatly impaired by shipping and harbor operations. In such a complex context, numerical simulation can be a powerful tool to complete the understanding achieved through experimentation, to analyse the potential area of plastics accumulation and to help local authorities in taking appropriate actions to prevent and retrieve plastics pollution from the marine environment.

The Bay of Biscay is considered as an area of accumulation of marine litter due to specific circulation patterns (Declerck et al., 2019; Gago et al., 2015; Lebreton et al., 2012). However, data on microplastics distribution and abundance in this region are scarce, as shown by the review of Mendoza et al. (2020). Data collected during the PE-LACUS survey in the southern Bay of Biscay highlighted a medium level of contamination at the sea surface, in comparison with other areas of the world (Gago et al., 2015). The Adour River provides the main

continental inputs for the coastal waters of the southeastern Bay of Biscay. Galgani et al. (2000) showed that the highest densities of litter on the sea floor in the Bay of Biscay were recorded in the area around the Adour Estuary. It was also suggested that the large amount of litter in Capbreton Canyon may be due to the proximity to the Adour Estuary. These observations raise the issue of the role played by the Adour Estuary in the contamination of coastal and regional waters by plastic litter, assumed to impact the rich local coastal ecosystems. The plastics load, including both micro-particles and larger litter, washed down by the Adour River into the Atlantic Ocean remains virtually unknown.

The main goal of the present paper is to analyse the microplastics distribution in a salt-wedge estuarine system, including typical abundance, vertical structure and tidal dynamics. The focus is placed on a series of fundamental issues which have to date been rarely addressed: can microplastics be found everywhere in the water column, especially during periods of intense mixing? To what extent is traditional surface sampling able to provide a correct estimation of fluxes? Is the estuarine contamination associated with the river discharge and the flushing efficiency? Are the local hydrodynamics responsible for specific dispersion processes? For example, could the salt-wedge displacement affect the microplastics distribution and abundance, as it does with suspended sediments? In order to achieve a better understanding regarding these issues, the present study combines field sampling and numerical modelling at a selected field site of a major importance for the southeastern Bay of Biscay: the Adour estuary, France. The main novelties of the study are the dynamic characterization of the in-situ contamination throughout the water column and the use of an Eulerian approach to numerically simulate the dispersion processes for both neutrally and negatively buoyant microplastic particles, which have to date been rarely documented.

## 2. Methods

### 2.1. Field site

The Adour Estuary is a time dependent salt-wedge estuary (Defontaine et al., 2018; Defontaine et al., 2019; Sous et al., 2018) in the southern Bay of Biscay. The present study focuses on the lower 10 km of the estuary fed by the Adour River and the Nive River. The mouth is well sheltered by a 700 m long jetty at the entrance, strongly reducing the wave energy propagating into the estuary (Bellafont et al., 2018). Wind effect is expected to be mostly weak, due to overall low wind exposure with day-averaged values of less than 5 m/s for 88% of time (1980–2017 statistics from Meteo France). The S shape of the lower estuary further reduces the influence of the wind in the estuary. The mouth of the estuary is forced by a mesotidal regime, with a mean tidal range of 2.5 m. Tidal signal is semi-diurnal and its four major harmonic constituents are M2, S2, N2 and K2. The river discharge is quite variable, with an annual mean of about 300 m<sup>3</sup>/s, summer low discharge below 80 m<sup>3</sup>/s and strong floods reaching more than 3000 m<sup>3</sup>/s for the most extreme events. The estuarine dynamics are characterized by strongly variable density and velocity fields, impacting the transport of particles in suspension (Defontaine et al., 2019). The rising tide is associated with strong vertical density stratification, while the falling tide undergoes intense mixing periods responsible for a horizontal density gradient. The watershed is nearly 17,000 km<sup>2</sup> mostly composed of urban, agricultural and industrial areas, with a total population of one million inhabitants. The lower estuary studied here comprises the port of Bayonne and is flanked by the cities of Bayonne, Anglet and Boucau, being potential sources of microplastic contamination. More than 160 outflows are present in the port area both from civil (e.g. Waste Water Treatment Plants - WWTP, sewage network, rainwater network, storm water overflows) and industrial sources, some of which releasing untreated wastewaters. The location of the WWTP discharges are indicated in Fig. 1 c).

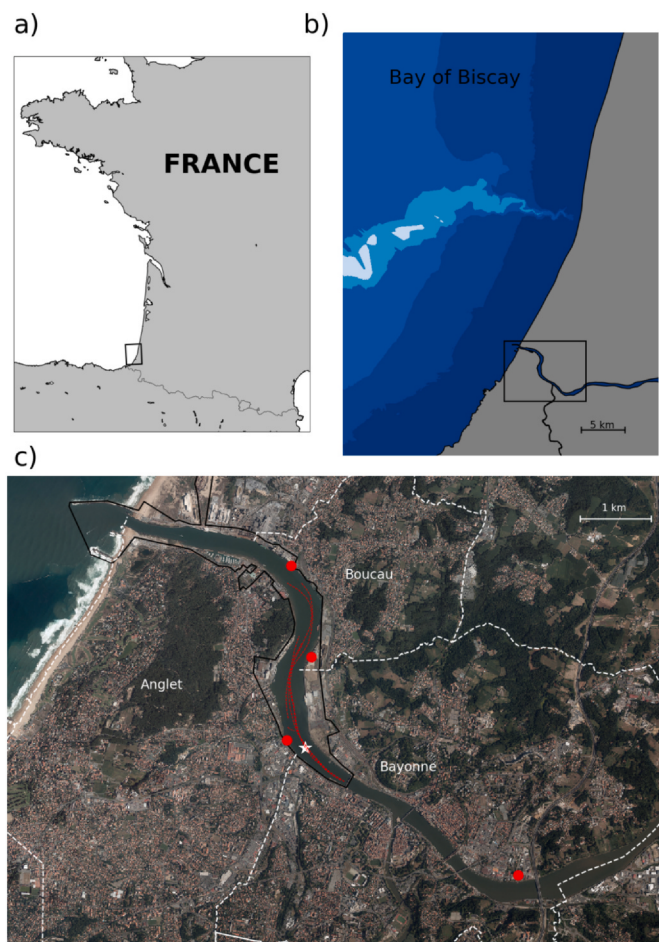


**Fig. 1.** Location of the Adour estuary on the SW Coast of France (a) and more precisely on the Basque Coast (b). Sample location in Adour Estuary (c). The white star represents the anchored boat station. The red dashed lines represent the manta trawl. The thick black line represents the Bayonne port area. The red dots indicate the location of WWTPs outflows. (For interpretation of the references to colour in this figure legend, the reader is referred to the web version of this article.)

## 2.2. Field sampling

Sampling was undertaken from an anchored boat about 5 km from the mouth of the estuary (Fig. 1 c)). This part of the estuary belongs to the port of Bayonne and is flanked by a densely populated urban area. Sampling was conducted on June 6th, 2019 during a flood event and on September 26th and 27th, 2019 during low river flow conditions. The river discharge rate was c.a.  $600 \text{ m}^3/\text{s}$  and  $85 \text{ m}^3/\text{s}$  during the June and September samplings, respectively. The river discharge rate was estimated based on continuous river discharge survey performed by the French Water Agency ([www.hydro.eaufrance.fr](http://www.hydro.eaufrance.fr)) for the Adour River and its tributaries. The tidal range was 3.3 m during June experiments and ranged from 2.6 m to 3.5 m during September experiments. The average wind magnitude and direction during the experiments were 4.1  $\text{m/s}$  at  $110^\circ$  on June 6, 3.4  $\text{m/s}$  at  $330^\circ$  on September 26 and 1.7  $\text{m/s}$  at  $180^\circ$  on September 27. The water surface was flat, except for episodic events of boat wakes.

Methodological strategies to sample microplastics in the field are still open to debate. While there appears to be a consensus on the maximum size limit of 5 mm, the minimum size limit is highly dependent on the sampling and analysis methods employed. In surface waters, a manta trawl equipped with a standard  $300\mu\text{m}$  net is generally used (Gallagher et al., 2016; Sadri and Thompson, 2014; Sutton et al., 2016; Yonkos et al., 2014; Zhao et al., 2014). Pumps may also be used

to collect water samples that are then filtered in the laboratory with different sieve and filter sizes, enabling microplastics of smaller size to be taken into account (e.g.  $45 \mu\text{m}$  (Xu et al., 2018),  $50 \mu\text{m}$  (Yan et al., 2019),  $63 \mu\text{m}$  (Gray et al., 2018)). There is a wide range of methods for quantification and identification as shown in the reviews of Hidalgo-Ruz et al. (2012) and Cutroneo et al. (2020). There is still a need for standardization of definitions, sampling methods and analysis in order to achieve a common perspective and to dispose of comparable data sets at worldwide scale.

The sampling approach adopted here combined surface measurements, using a classical trawl net, with subsurface and near-bottom measurements using an immersed pump. For both measurement systems, the sampling duration and the related sampled volume were strongly constrained by two conflicting requirements. On one hand, large volumes would allow more statistically robust results. On the other hand, the sampling duration is limited by the need to resolve in time the microplastics dispersion along the tidal cycle. The aim is to obtain successive samples over the tidal cycle representing a series of snapshots of the estuarine water contamination at different stages of the tidal cycles. The Adour Estuary is a tidally-driven intermittent salt-wedge estuary where strong variations in current properties (magnitude, direction, vertical shear, turbulent mixing) and density structure (potentially varying from fully filled by fresh or marine waters to a wide range of vertical density stratification patterns) can be observed. Each stage of the tidal cycle is therefore characterized by specific local hydrodynamic properties which are likely to affect the local microplastics contamination. The selection of the sampling duration was therefore intentionally limited to 30 min in order to capture the temporal estuarine patterns of change driven by tide and salt-wedge dynamics. The assumption is thus made that, for each sample, the hydrodynamic conditions can be considered as quasi-stationary. In addition, some of the sampling was interrupted before the targeted duration by port authorities for shipping purposes or by collisions with large sized floating litter. For the same reason, only the ebbing to low tide has been documented during the high discharge sampling (June) while a more complete description has been undertaken during the September experiment. These constraints finally result in sampling durations between 10 and 30 min for both sampling methods described hereafter, namely the Manta net surface sampling and the subsurface and near bottom water pumping. Due to strong differences in sampling flux between surface net trawling and water pumping, this leads to wide differences in sampled volumes.

### 2.2.1. Manta net sampling

Surface water microplastics were collected with a manta trawl net with a rectangular opening 15 cm high by 30 cm wide, and a  $300 \mu\text{m}$  mesh net. The net immersion was controlled by the lateral wings in such a way that 10 cm of the net mouth was underwater. Immersion depth fluctuations were visually estimated at about 2 cm. Typical sampling duration was 30 min with a tow speed of 2 to 3 knots relatively to the water mass. The Manta net towing tracks followed approximately the main channel of the estuary, but differ in length due to the variability of surface current conditions. In a number of cases, the sampling was stopped either when the trawl mouth was obstructed by plant debris, branches or other macro-litter or when imposed by the port authorities. Samples with a duration of less than 10 min were discarded from the analysis. The manta trawl was equipped with a mechanical flowmeter to estimate the flow velocity, allowing calculation of standardized values per cubic meter. The sampled volumes varied from 45 to  $146 \text{ m}^3$  with a relative uncertainty of about 20 % due to small fluctuations in the immersion depth. Surface conductivity and temperature were measured (van Essen CTD-diver probe sampling at 1 Hz) for each sample to estimate local salinity.

### 2.2.2. Water pumping

Subsurface and bottom water were sampled with a 750w immersed

pump. Before each sampling, the pump discharge at the selected depth was first calibrated by timing the filling of a 0.5 m<sup>3</sup> tank. The pump, weighted by 20 kg of lead, was positioned either in subsurface, i.e. approximately 1 m below the free surface, or in the near-bottom layer, i.e. approximately 1 m above the river bed. Due to the strong current, total control of the immersion depth was impossible but for each case the actual sampling depth was measured with an embedded pressure sensor (van Essen CTD-diver® sampling at 1 Hz). Conductivity and temperature were also measured with the same probe for each sample to estimate local salinity at the depth reached. The pumped water was poured through two successive sieves of 5 mm and 300 µm in order to provide pre-sorted samples. The pumped volume varied from 2.8 to 5.1 m<sup>3</sup>.

### 2.3. Analysis

After sampling, additional separation is required to identify and quantify microplastics from the water samples. Recent reviews show that the most common techniques are visual sorting, density separation and filtration which can be combined to varying degrees or completed by finer analysis such as Fourier-Transform Infrared Spectroscopy (Alvim et al., 2020; Cutroneo et al., 2020). The identification is performed here by visual inspection and separation using a binocular magnifier (Leika M165C) and metal tweezers. Used alone, this approach would be inappropriate for microplastics below 100 µm [(Lenz et al., 2015)]. For the size range studied here (> 300 µm), polymer particles are generally straightforward to discriminate from mineral or vegetal particles by an experienced operator on the basis of brightness, hardness, stiffness and absence of striation (Covernton et al., 2019). Recent intercomparisons provided an estimation of the related identification uncertainty, of about 14 % (Gadiou et al., 2020). Each sample was sorted on a petri dish, the microplastics isolated and finally dried in an oven at 45 °C during 24 h. Microplastic characterization was performed by imaging. Dried fragments were digitally recorded with a Zooscan device. After this, counts and maximum length were determined through Image J and Plankton identifier. Microplastics were classified into five categories of shape, namely spheres, fibers, fragments, films and others.

### 2.4. Numerical model

#### 2.4.1. Hydrodynamics

The simulations were run with a TELEMAC-3D numerical model from the open source TELEMAC-MASCARET® modelling system. TELEMAC-3D solves the free surface Navier-Stokes equation (Hervouet, 2007). The hydrostatic pressure hypothesis and the Boussinesq approximation on the density were taken into consideration in the momentum equation. The turbulent closure model is based on a turbulent viscosity concept using the Prandlt formulation of the mixing length theory. The Munk Anderson damping function, decreasing with the value of the Richardson number, was used to reproduce the damping of turbulent mixing due to density stratification. An unstructured triangular mesh was created on Blue Kenue® covering the Basque country coast and the Adour and Nive Rivers, with cells from 30 m to 2000 m (Fig. 2). The finest resolution (30 m cells) was inside the lower Adour Estuary (i.e. corresponding to the field experimentation site). The grid covered the ocean up to 40 km from the estuary mouth and it extended up to 70 km in the Adour and 25 km in the Nive River. The vertical dimension was resolved with 20 equidistant sigma coordinate layers. At the marine boundary, tidal forcing was imposed at each node using 11 harmonic constituents of the TPXO data base. The tidal range imposed during the simulations was 3.5 m, i.e. close to the field conditions. At both riverine boundaries, a river discharge was forced. Two river flow conditions were considered to mimic the field conditions: low river flow corresponding to the September sampling, with the Adour and Nive Rivers flow of 90 and 10 m<sup>3</sup>/s, respectively, and high river flow

corresponding to the June experiment, with the Adour and Nive Rivers flow of 525 and 75 m<sup>3</sup>/s, respectively. No wind or wave forcing was considered in the present simulations. The initial conditions consist in the last time step of a previous computation of 25 days sufficient to establish the flow and the salinity structure (Defontaine, 2019). The model was calibrated and validated based on tidal gauge data (five gauges), two bottom-moored ADCP data and density profiles collected in 2017 and 2018; for further details refer to Defontaine (2019).

#### 2.4.2. Microplastics dispersion

Microplastics were treated as passive tracers with concentrations that changed with time and space by solving the advection-diffusion equation with an additional settling velocity. The turbulent diffusion coefficient of microplastics is assumed to be the same as for turbulent momentum diffusion, i.e. corresponding to a turbulent Schmidt number of 1. Three types of particles were considered for simulations to explore the effect of mean diameter, density and settling velocity on the dispersion. The parameters used in S1 and S2 simulations (see Table 1) are typical values recovered from laboratory measurements presented in the literature: S1 is representative of a polystyrene sphere of 0.5 mm (density = 1.05 g/cm<sup>3</sup>) (Kowalski et al., 2016) and S2 is representative of a polycaprolactone sphere of 4.9 mm (density = 1.13 g/cm<sup>3</sup>) (Khatmullina and Isachenko, 2017). For simulation S3, an idealized neutrally-buoyant particle of 3 mm is considered with a density equal to fresh water density.

#### 2.4.3. Simulation runs

Each model run was 9 days long. In order to understand the dispersion of microplastics in a time-dependent density-stratified water mass, a single patch of microplastics was released at a given point of the lower estuary on day 4 at high tide during 15 min, with a concentration of 10 g/L. The source was located on the right bank at the level of Bayonne city (Fig. 2), at zero meters above the chart datum. Each type of simulation was run twice, in high and low river flow conditions, amounting to 6 simulations. Four Eulerian control points were used to monitor the changes over time in concentrations, see Fig. 2. C1 was located at the river mouth to analyse exchanges with the ocean, C2 was in front of the initial release point and C3 and C4 were upstream in the Nive River and Adour River, respectively, to monitor the time-varying microplastics distribution.

#### 2.4.4. Numerical products

In addition to the direct analysis of concentrations, the numerical results were processed using two non-dimensional numbers, namely the Richardson number and the Rouse number.

The Richardson number  $Ri$  estimates the relative importance of the gravitational effects induced by the density gradient and the vertical shear on the stability of the water column. It is expressed as:

$$Ri = -\frac{N^2}{S^2} \quad (1)$$

where  $N^2 = -\frac{g}{\rho_0} \partial \rho / \partial z$  is the Brunt-Väisälä frequency,  $g$  is the gravity acceleration,  $\rho_0$  is the reference density and  $S = \partial \bar{u} / \partial z$  is the vertical shear of the mean horizontal velocity. The buoyancy forces induced by the vertical density gradient are assumed to overcome turbulent mixing due to shear stress when the Richardson number is above the threshold value of 0.25. By contrast, an unstable configuration induced by the stratification breakdown by the turbulent mixing is expected for values of the Richardson number below 0.25.

The Rouse number  $Ro$  is defined as the ratio of the settling velocity to the shear flow:

$$Ro = \frac{w_s}{\kappa u^*} \quad (2)$$

where  $w_s$  is the settling velocity,  $\kappa$  is the Von Karman's constant and  $u^*$  is the shear velocity. It is generally used to determine the mode of

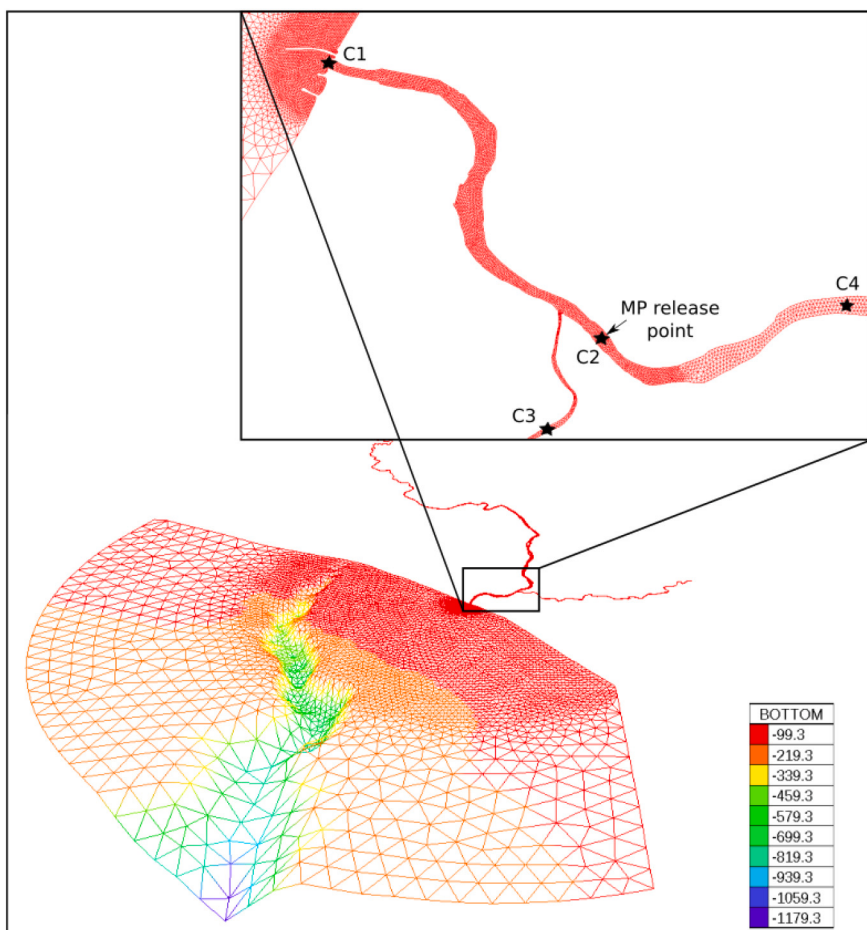


**Fig. 2.** 3D view of the mesh grid, with a top-view zoom on the lower part of the estuary where the measurements took place, colours corresponding to the bed level in meters. The black arrow shows the location of numerical microplastics release. C1 to C4 are control points where simulated concentrations of microplastics are retrieved for data analysis.

**Table 1**  
Microplastic characteristics used for simulations.

Simulation name	Mean diameter (mm)	Density (g/cm <sup>3</sup> )	Settling velocity (mm/s)
S1	0.5	1.05	4
S2	4.9	1.13	127
S3	3	1.00	0

sediment transport with several thresholds: bed load ( $Ro > 2.5$ ), 50% suspended ( $1.2 < Ro < 2.5$ ), 100% suspended ( $0.8 < Ro < 1.2$ ) and wash load ( $Ro < 0.8$ ).

### 3. Results

#### 3.1. Field observations

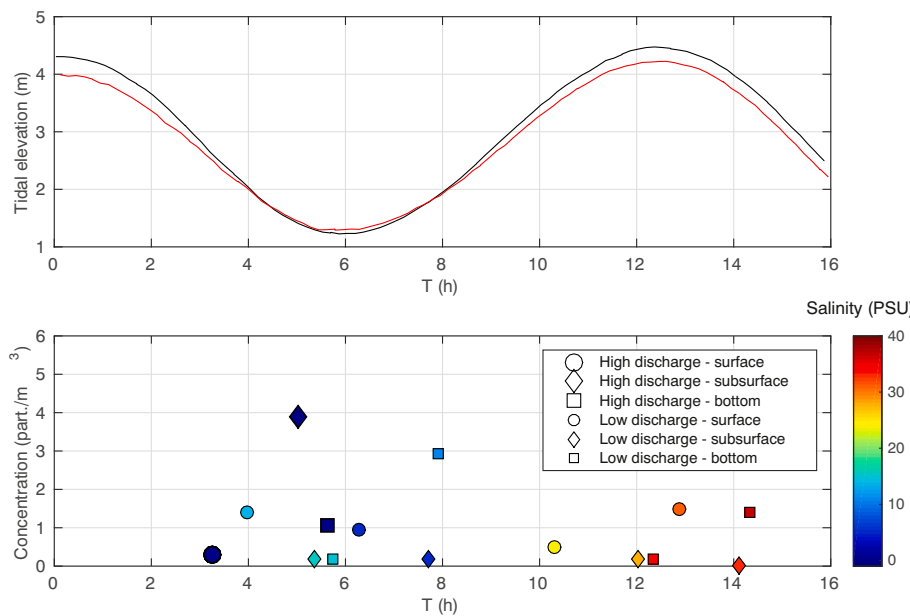
A total of 669 microplastic particles were collected during this study. Only one sample out of a total of fifteen (6.7%) was free of microplastics. The average number of microplastics per sample was 126 for trawl and 4 for pumped sampling, respectively, reflecting the difference in sampled volumes. Concentration of microplastics found in the samples ranged from 0 to 3.88  $\text{part}/\text{m}^3$ , with a mean and median abundance of 1.13 and 0.81  $\text{part}/\text{m}^3$  (standard deviation 1.12  $\text{part}/\text{m}^3$ ).

A first striking observation is that microplastics were present throughout the water column with similar levels of contamination. Mean abundance for surface and subsurface layers over both discharge conditions were 1.18 and 0.89  $\text{part}/\text{m}^3$ , respectively. Corresponding median values and standard deviations are 0.94 and 0.98  $\text{part}/\text{m}^3$  for the surface layer and 0.2 and 1.67  $\text{part}/\text{m}^3$  for the subsurface layer. The

highest mean abundance of 1.26  $\text{part}/\text{m}^3$  was found near the bottom waters, with a median value of 1.23  $\text{part}/\text{m}^3$  and a standard deviation of 1.04  $\text{part}/\text{m}^3$ .

High river flow was associated with higher depth-averaged concentration (mean of 1.60, median of 1.41 and standard deviation of 1.28  $\text{part}/\text{m}^3$ ) than low discharge conditions (mean of 0.96, median of 0.58 and standard deviation of 1.06  $\text{part}/\text{m}^3$ ). This is probably due to a combination of several factors, including higher land and city drainage during flood and/or sewage treatment plants discharge. It should be stressed that even if the overall order of magnitude for the concentration remained within the same range, the difference in river discharge between the June and September experiments led to a much stronger net export flux for the high discharge conditions.

The tidal evolution of microplastics concentrations through the water column are presented in Fig. 3. Salinity values showed that, during low discharge conditions, the estuary was filled with riverine fresh/marine salty waters around low/high tide, respectively. A small vertical density stratification was present at rising tide for low discharge condition, see the salinity gradient just before 8 h between subsurface (diamond,  $S = 4.9$ ) and bottom (square,  $S = 10.8$ ) measurements. For high discharge conditions (large symbols), marine waters were totally expelled from the estuary during the ebb tide. For more detailed information on the estuarine hydrodynamics, the reader can refer to (Defontaine et al., 2019). Fig. 3 first reveals that, in most cases, the microplastics concentration fluctuated between 0.2 and 2  $\text{part}/\text{m}^3$  regardless of the discharge and tidal conditions, the ambient salinity and of the position in the water column. This consolidates the mean order of magnitude previously mentioned. The identification of finer trends, either over time or through the water column was not straightforward. Two peaks of concentration were however observed



outside this typical range. The first was for high discharge conditions at the end of the ebb, where subsurface concentrations were observed at 3.9 part/m<sup>3</sup> and the second at 2.9 part/m<sup>3</sup> was observed in the near bottom layer at the beginning of the rising tide in low discharge condition. While these peaks could have been caused by a number of factors including variation in external inputs, the local hydrodynamics could play a significant role in the peak development. Defontaine et al. (2019) have shown that late ebb corresponds to a peak of velocity and turbulent mixing responsible for massive sediment resuspension events reaching the surface. This could affect the concentration of microplastics in a similar manner, as observed by the former peak of microplastics concentrations (3.9 part/m<sup>3</sup>). The latter peak (2.9 part/m<sup>3</sup>) could be attributed to the deposition mechanism observed at the beginning of the rising tide when a minimum of velocity is reached (i.e. current reversal) (Defontaine et al., 2019).

Fig. 4 depicts the shape (a) and size (b) distributions of the sampled microplastics. Films and fragments were the predominant types of microplastics found in the lower Adour Estuary, respectively 59.6% and 22.3%, followed by spheres found at 12.6%. The form distribution in the surface was similar to the depth-averaged one, reflecting the difference in sampled volumes. In subsurface layer, fragments were clearly

**Fig. 3.** Tidal evolution of microplastics concentrations for low and high discharge events. Top: tidal elevation for low (September, in red) and high (June, in black) discharge conditions. Bottom: measured concentrations for low (small symbols) and high (large symbols) discharge conditions. Surface, subsurface and bottom measurements are denoted by circles, diamonds and squares, respectively. The ambient salinity (PSU) at the sampling depth is shown by the colour level. (For interpretation of the references to colour in this figure legend, the reader is referred to the web version of this article.)

predominant while fibers were absent. In the bottom layer, fragments showed similar levels to films, with a small proportion of fibers and spheres.

The size distribution (Fig. 4 right panel) was also depth-variable. Surface distribution was the most balanced with the 0.5–1, 1–2 and 2–3 mm classes sharing about 75% of the particles. The subsurface layer was characterized by the absence of very fine (0.3–0.5 mm) particles and the clear dominance of the 1–2 mm class while an overall shift toward finer particles was observed near the bottom.

### 3.2. Numerical results

A series of numerical simulations have been performed to provide further insight on the spatial and temporal dynamics of microplastics with variable properties, see Table 1. The objective was to track the dispersion of a single patch of microplastics released at a source point during a short time period. The following analysis was based on a longitudinal section of concentrations, salinity, Richardson number and Rouse number at mid falling and rising tides for the three types of particle for low and high river discharge conditions (Figs. 5 and 6, respectively), tidal evolution of water column stability (Richardson

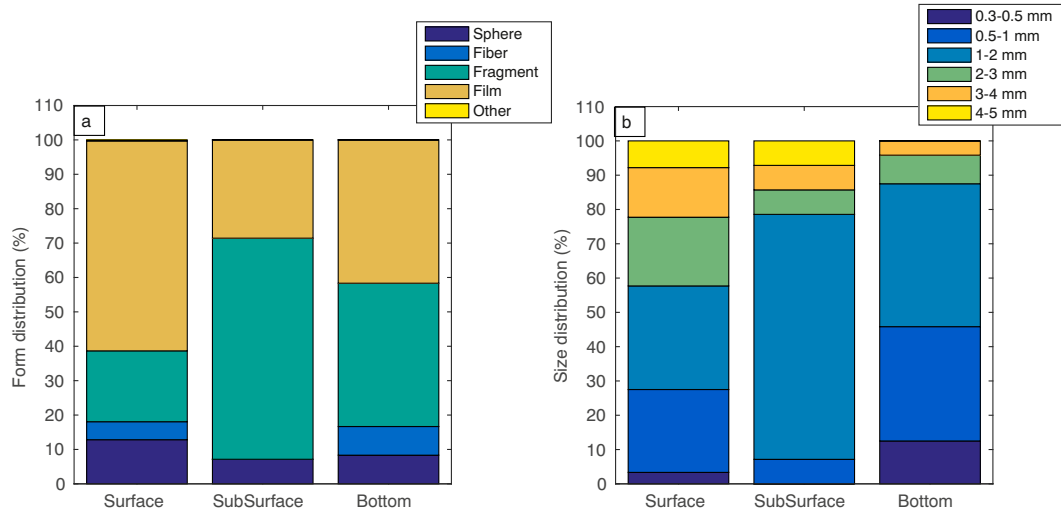


**Fig. 4.** Distribution of forms (a) and sizes (b) of the sampled microplastic particles in surface, subsurface and bottom layers.

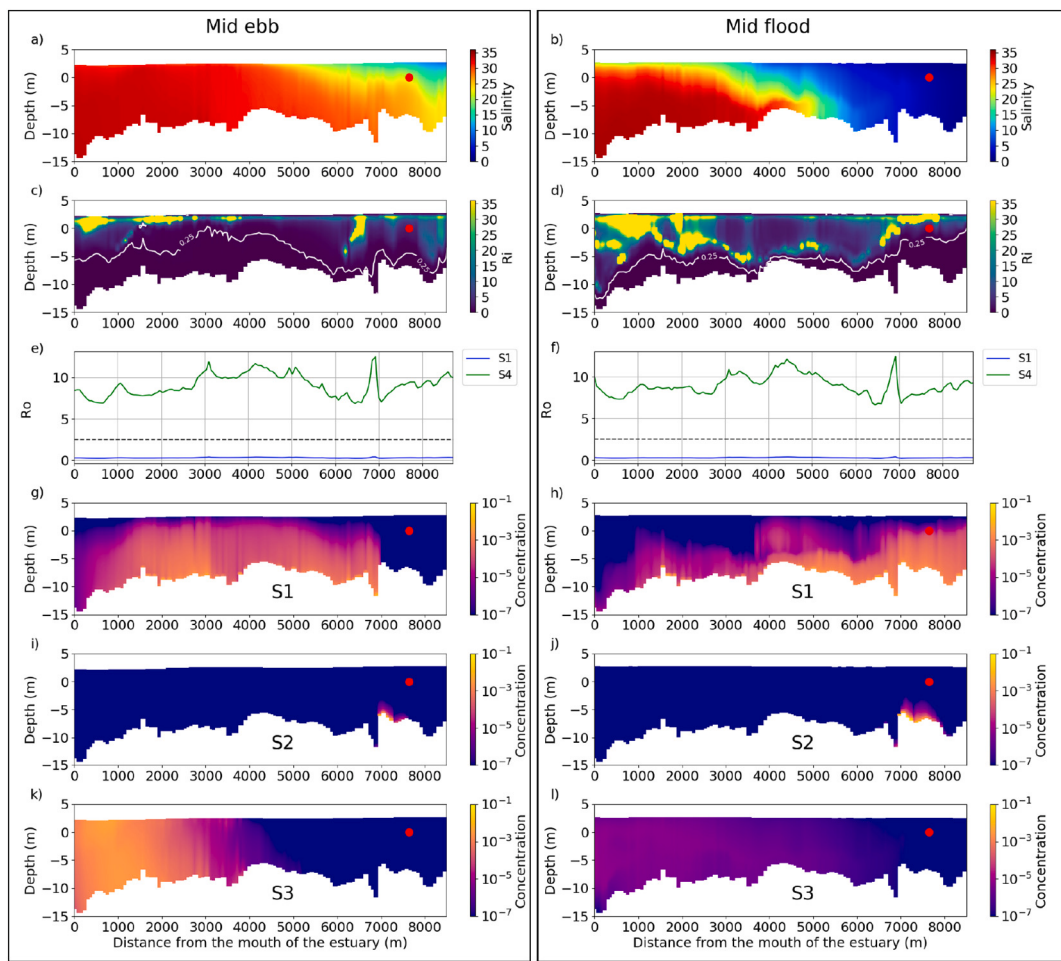


**Fig. 5.** a) and b): longitudinal section of salinity at mid falling and rising tides. c) and d): longitudinal section of the Richardson number, the white line indicates the threshold value of  $Ri = 0.25$  between stable and unstable configurations. e) and f): time series of Rouse number for the simulation S1 (blue) and S2 (green), the dashed line indicates the threshold value of  $Ro = 2.5$  between bed load transport and transport in suspension. g) to l): longitudinal section of microplastics concentrations in g/L for the three simulation runs (S1, S2 and S3). Data were extracted about 3 h (mid ebb = left panel) and 9 h (mid flood = right panel) after the microplastic release on Day 4 under low river discharge conditions. On longitudinal sections the red dot indicates the location of the microplastics release.

number) and transport capacity (Rouse number) for the S1 case (Fig. 7) and time evolution of concentrations at four selected control points in the estuarine system during low and high river discharge conditions (Figs. 8 and 9, respectively).

Microplastics, like any particle in suspension, are very sensitive to hydrodynamics. Therefore, tidal currents are of the utmost importance for the transport of microplastics in suspension. Microplastics were transported in an oscillating manner, upstream and downstream in the estuary following the tidal motion (Figs. 8 and 9). The patch of microplastics moved downstream during the falling tide and upstream during the rising tide. One part of the microplastics patch moved into the Nive River during the rising tide. Thus, the Nive River could become contaminated by microplastics released into the Adour River. Different peaks of concentration can be observed in Figs. 8 and 9.

Defontaine (2019) showed that peaks of sediment concentrations are correlated with periods of maximum velocity and peaks of turbulent mixing. A similar pattern of behaviour for microplastics is confirmed by the present numerical results. Focusing on S1 simulation with microplastics heavier than marine water and having a low settling velocity (Fig. 5 g) and h) and Fig. 6 g) and h), the salinity field strongly affects the resuspension mechanism. During the rising tide, the strong density stratification typical of the salt-wedge structure damps the turbulent mixing and thus contains the transport in suspension below the pycnocline (Figs. 5 h) and 6 h)). During the falling tide, the typical periods of intense mixing led to greater vertical spreading and more

homogeneous concentration through the vertical (Figs. 5 g) and 6 g)). These alternating periods of resuspension/deposition over the tidal cycle are clearly visible in Fig. 7. At the end of the ebb tide, the water column is unstable ( $Ri < 0.25$ , i.e. periods of intense mixing), favoring the transport of microplastics in suspension ( $Ro < 2.5$ ) throughout the whole water column (i.e. high concentration of microplastics at the surface). At the beginning of the rising tide, the water column is well-mixed ( $Ri < 0.25$ ), but the current reversal is associated with a strong reduction of the transport capacity ( $Ro > 2.5$ ) inducing microplastics deposition on the bed. At mid flood tide, the salt-wedge entrance results in a highly stratified and stable water column. The resuspension is thus contained by the pycnocline with a drop in mid and surface concentrations. At the end of the flood tide, the peak of the Rouse number indicates the reversal of the current and its associated deposition process.

Microplastics transport was also affected by their inner characteristics: size, density and associated settling velocity. Neutrally-buoyant microplastics easily spread through the entire water column and they were more affected by tidal flushing (Figs. 8 c and 9 c). They were flushed from the estuary within few tidal cycles, while heavier microplastics tend to stay in the estuary. The good flushing capacity of neutrally-buoyant microplastics can be explained by the actions, during the rising tide, of a two-layer flow with marine waters entering into the estuary bottom layers and riverine waters flowing out of the estuary at the surface and, during the falling tide, an outflow of the full water

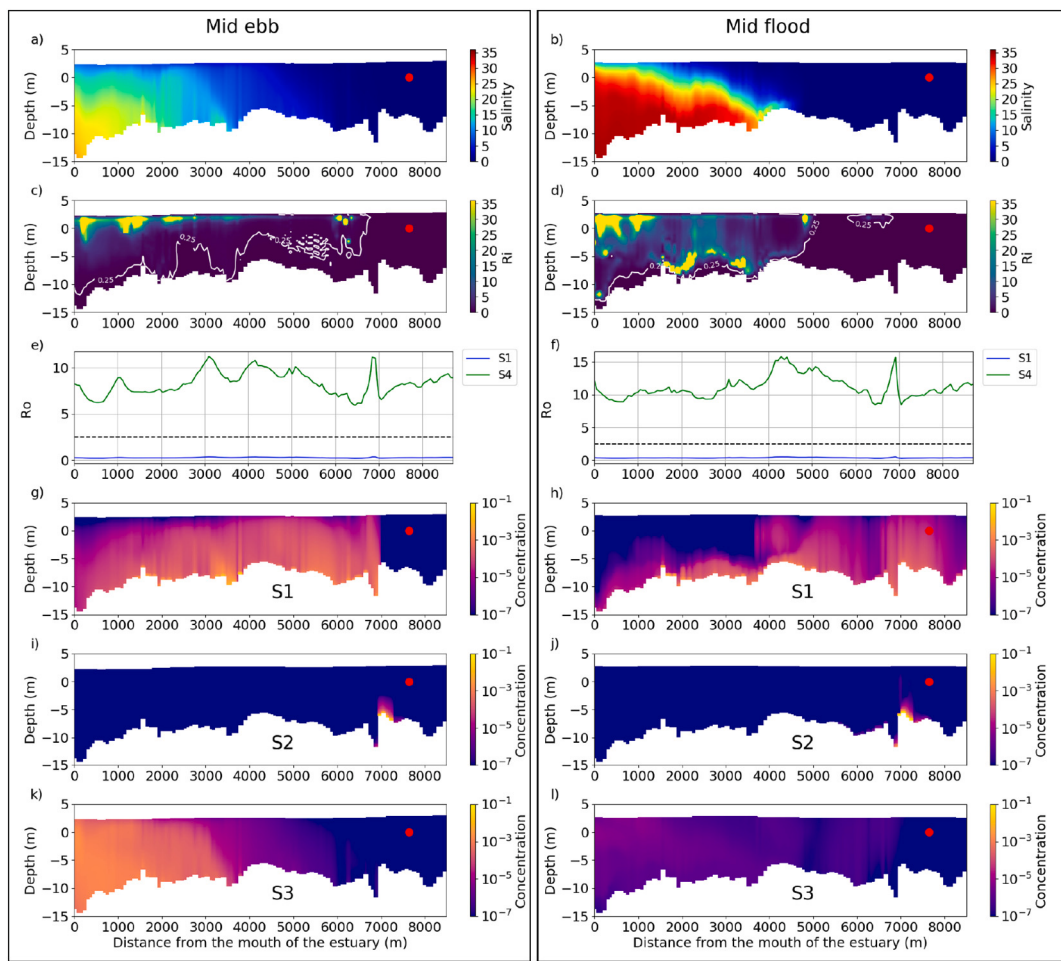


**Fig. 6.** a) and b): longitudinal section of salinity at mid falling and rising tides. c) and d): longitudinal section of the Richardson number, the white line indicates the threshold value of  $Ri = 0.25$  between stable and unstable configurations. e) and f): time series of Rouse number for the simulation S1 (blue) and S2 (green), the dashed line indicates the threshold value of  $Ro = 2.5$  between bed load transport and transport in suspension. g) to l): longitudinal section of microplastics concentrations in g/L for the three simulation runs (S1, S2 and S3). Data were extracted about 3 h (mid ebb = left panel) and 9 h (mid flood = right panel) after the microplastic release on Day 4 under high river discharge conditions. On longitudinal sections the red dot indicates the location of the microplastic release.

column. The surface waters are thus almost permanently flowing out the estuary. Neutrally-buoyant microplastics being generally more concentrated in the surface layer than heavier microplastics, their residence time is reduced. Microplastics with a density higher than that of marine water but a low settling velocity (S1) spread along the Adour and Nive Rivers (i.e. from C1 to C4), with a gradient of concentration from surface to bottom (Figs. 8 and 9 a, d, g and j). Microplastics leaving the estuary during the ebb were re-injected by coastal waters during the following flood tide. This re-injection of microplastics during the rising tide is partly due to the fact that longshore currents, wave and wind forcing in the coastal area were not considered in the simulations. Dense microplastics with a high settling velocity (S2) sank at the level of the source point. They just moved back and forth over a short distance close to the source point. They were re-suspended and deposited by the salt-wedge displacement, but they were never flushed out of the estuary.

The difference between low and high river flow conditions is straightforward in Figs. 8 and 9. Microplastics flushing was faster with high river flow and the upward displacement of microplastics was reduced. In simulations S2 and S3, microplastics were not able to reach the C4 control point during the rising tide under high river flow (Fig. 9). In simulation S1, the concentrations at C2, C3 and C4 clearly decreased with time during high river flow conditions. The higher concentrations of microplastics were localised at the entrance of the estuary (i.e. C1 and C2), while during the low river discharge the higher concentrations

were upward at C3 and C4. This pattern was similar to that of an estuarine turbidity maximum (ETM), which generally moves downstream during high river flow and upward during low river flow (Burchard et al., 2018).

#### 4. Discussion

Discussion points are organized in four main topics: microplastics abundance and fluxes, influence of microplastics properties on their dispersion, influence of the salt-wedge dynamics on microplastics dispersion and simulation hypothesis and limitations.

##### 4.1. Microplastics abundance and fluxes

The present field sampling provided the first estimation of microplastics abundance in the Adour Estuary with a mean value of  $1.13 \text{ part/m}^3$ . For the sake of comparison, microplastics contamination levels reported in other estuaries are summarized in Table 2. European estuaries have lower to comparable levels of contamination, while field studies in Asia and USA reported higher values of contamination, up to four orders of magnitude higher. Note also that the microplastics abundance in the Adour estuary is similar to the subsurface water abundance in the Bay of Biscay. Nevertheless, inter-site comparisons should be undertaken with caution due to the lack of standardization regarding the definition of microplastics, particularly regarding the size

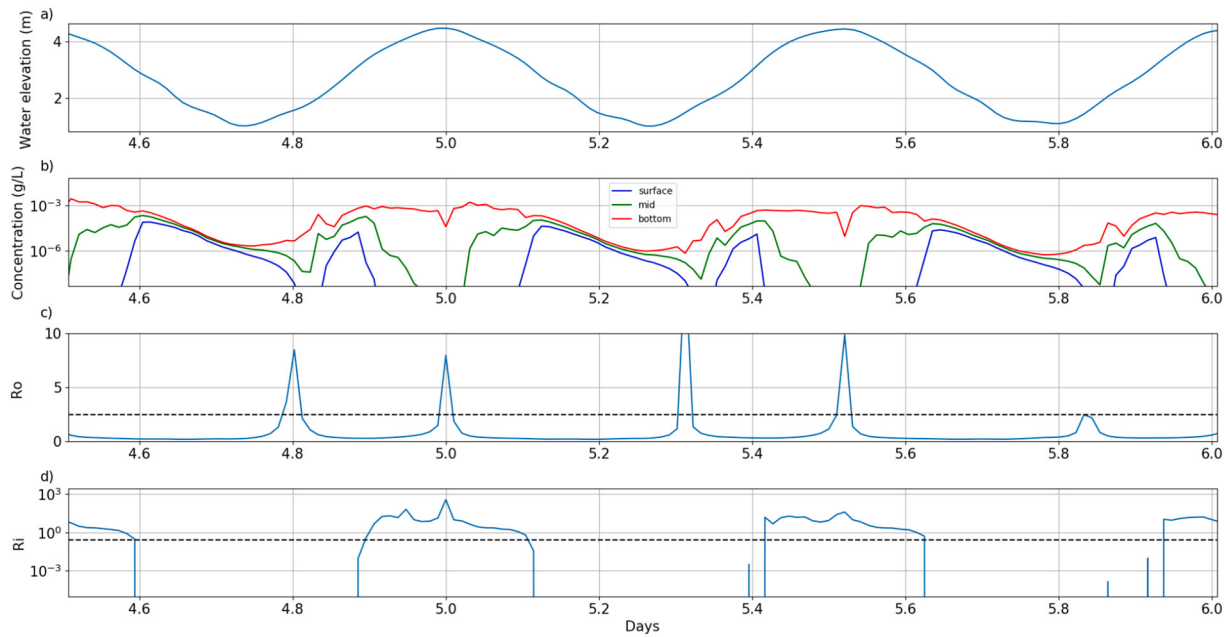


**Fig. 7.** Time series of a) water elevation (m), b) microplastics concentrations (g/L), c) Rouse number and d) vertically averaged Richardson number. The dashed lines indicate the threshold values for the Rouse number  $Ro = 2.5$  and the Richardson number  $Ri = 0.25$ . Data were extracted from S1 simulation in high river flow conditions at the C2 control point.

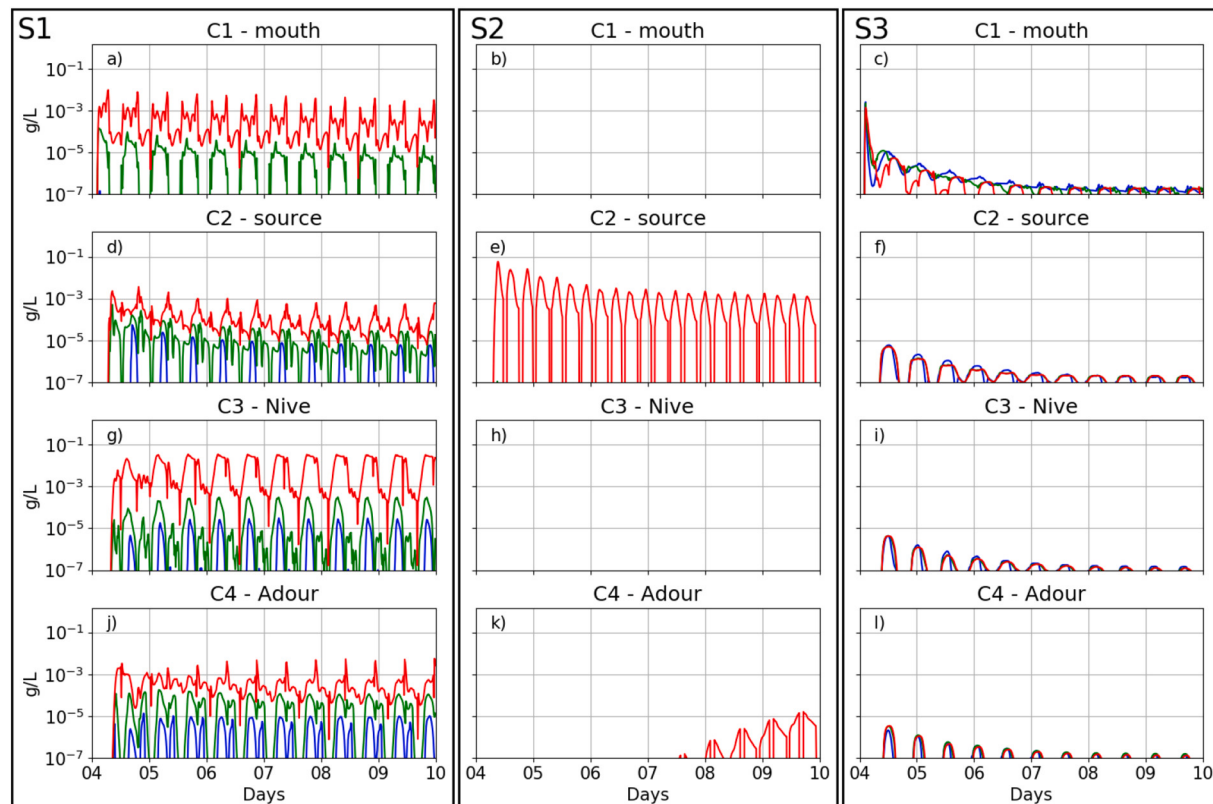


**Fig. 8.** Concentrations in microplastics during low river discharge condition. The four rows correspond to the four control points: C1 (mouth of the estuary), C2 (close to numerical release point), C3 (upstream Nive River) and C4 (upstream Adour River). The three columns correspond to the three types of simulated particles: S1 for (a, d, g, j), S2 for (b, e, h, k) and S3 (c, f, i) and l)). Red, green and blue lines correspond to bottom, mid-column and surface concentrations (g/L), respectively. (For interpretation of the references to colour in this figure legend, the reader is referred to the web version of this article.)

and the sampling techniques. Apart from the methodological issue of collection techniques discussed previously, the difference in contamination levels between estuaries is likely due to anthropogenic pressure which can be approximated with the size and the use of the

watershed and the size of adjacent urban areas. Microplastics pollution is significantly correlated with the proximity to and the size of urban areas (Gago et al., 2015; Lebreton et al., 2017; Naidoo et al., 2015; Rodrigues et al., 2019; Yonkos et al., 2014).

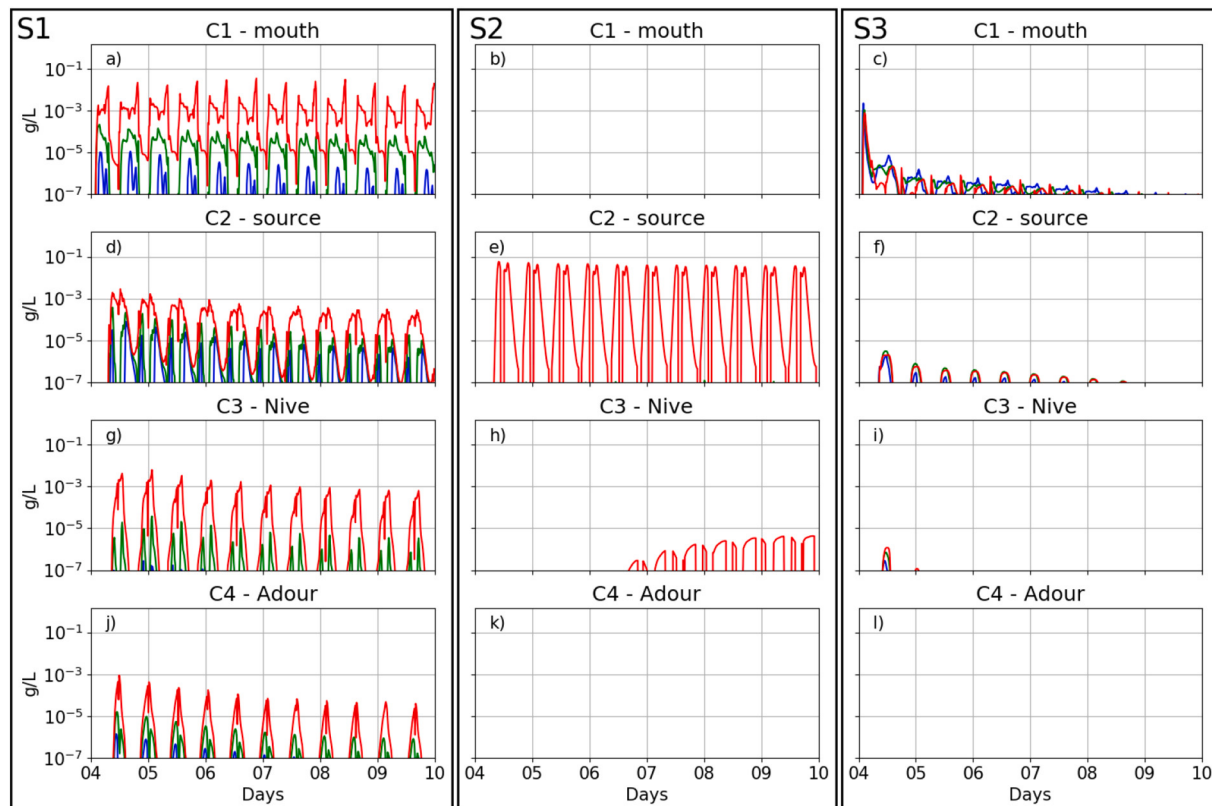


**Fig. 9.** Concentrations in microplastics during high river discharge condition. The four rows correspond to the four control points: C1 (estuary mouth), C2 (release point), C3 (upstream Nive River) and C4 (upstream Adour River). The three columns correspond to the three types of simulated particles: S1 for (a), d), g), j), S2 for (b), e), h), k) and S3 (c), f), i) and l)). Red, green and blue lines correspond to bottom, mid-column and surface concentrations (g/L), respectively. (For interpretation of the references to colour in this figure legend, the reader is referred to the web version of this article.)

Microplastics have been found throughout the water column of the lower Adour Estuary, for nearly each river discharge condition and tidal stage. Highest concentrations close to the river bed demonstrated the importance of estimating the microplastics abundance throughout the water column in estuaries. To limit microplastics studies to an estimation of surface abundance may therefore lead to serious underestimation of the plastics contamination and fluxes. For instance, simple estimates of daily fluxes as the product of the mean concentration with the river discharge led to values of around 7 and 110 million microplastic particles exported each day toward the ocean for low and high discharge conditions, respectively. The assumption that the total daily flux can be approximated by the surface layer flux captured by the Manta net would lead to values about two orders of magnitude lower, i.e. respectively to 0.07 and 1 million microplastics. It should be additionally emphasized that a fine estimation of exported fluxes in a salt-wedge estuary would require higher resolution and extension in the sampling protocol, allowing better characterization of the variation of contamination in time and space in the presence of time-dependent density stratification and its associated two-layer flow. The tidal oscillations of the estuarine waters and the vertical structure of the current, with opposite flows during the salt-wedge passage, require an extensive characterization of the concentration and current profiles throughout the tidal cycle to provide relevant estimations of exported fluxes.

#### 4.2. Influence of microplastics properties on their dispersion

The present study has shown that the distribution of the different types of microplastics through the water column is not homogeneous. This could be due to different sources, dispersion patterns and residence times. The predominance of films and fragments in the Adour Estuary over other kinds of shapes (fibers, spheres and other) suggests that

microplastics are of a secondary source (i.e. decomposition of larger items) rather than direct inputs of industrialized pellets or microspheres. Fibers represented a moderate contribution to the Adour Estuary contamination. However, fibers were predominant in sub-surface waters and in the beach sediments of the Bay of Biscay (Lusher et al., 2014; Masiá et al., 2019). This may suggest that heavier microplastics may be retained in the estuary or adjacent beaches, while fibers are able to easily flow offshore. Fibers can also have marine-based sources, i.e. fishing activities.

Simulations confirmed that microplastics properties play an important role with regard to the abundance and distribution of microplastics in estuaries, as well as on the flushing capacity. Neutrally-buoyant microplastics spread throughout the water column, while heavier microplastics are contained in the lower part of the water column. As a result, neutrally-buoyant microplastics are more easily flushed than heavier ones. Heavy particles are trapped inside the estuary and are therefore prone to accumulation. Field sampling revealed that near-bottom particles tend to be finer than surface ones. The hypothesis can be proposed that heavy particles trapped in the estuary are exposed to longer residence time and therefore increased degradation and fragmentation. This may partly explain why bottom microplastics sampled in the field are finer than those retrieved in the surface layer. Further density and settling velocity analysis should be performed to confirm this assumption. Overall, the numerical results confirm that all microplastics can not be considered as having the same behaviour. Three typical types of particles have been tested by the present simulations in order to provide clear discrimination between dispersion patterns. The range of tested particles will be extended in the future, including in particular the particle properties extracted from the field samplings.

**Table 2**  
Reported microplastics abundance for estuaries around the world and the Bay of Biscay.

Location	Mean concentration (part/m <sup>3</sup> )	Depth	Sampling method	Size	Reference
Tamar Estuary (UK)	0.028	Surface	Manta net	[300 µm - 5 mm]	Sadii and Thompson (Sadii and Thompson, 2014)
Douro Estuary (Portugal)	0.17	Subsurface (1–2 m)	Conical	[30 µm - 500 µm]	Rodrigues et al. (Rodrigues et al., 2019)
Ebro Estuary (Spain)	3.5	Surface	Neuston net	[5 µm - 5 mm]	Simon-Sánchez et al. (Simon-Sánchez et al., 2019)
Changjiang Estuary (China)	231	Subsurface (50 cm)	Pumping	[70 µm - 5 mm]	Xu et al. (Xu et al., 2018)
Minjiang Estuary (China)	1246	Subsurface (30 cm)	Pumping	[333 µm - 5 mm]	Zhao et al. (Zhao et al., 2015)
Yangtze Estuary (China)	4137	Subsurface (1 m)	Pumping	[32 µm - 5 mm]	Zhao et al. (Zhao et al., 2014)
Pearl Estuary (China)	8902	Surface	5 L water sampler	[50 µm - 5 mm]	Yan et al. (Yan et al., 2019)
Winyah Bay (USA)	30,800	Subsurface (3 m)	Sea surface microlayer collection apparatus	[63 µm - 2 mm]	Gray et al. (Gray et al., 2018)
Bay of Biscay	2	Subsurface (3 m)	Pumping	[250 µm - 5 mm]	Lusher et al. (Lusher et al., 2014)
Northeastern Atlantic	2.46	Subsurface (3 m)	Pumping	[250 µm - 5 mm]	Lusher et al. (Lusher et al., 2014)
Western Coast of Portugal Bay of Biscay	3.5	Subsurface (1.1 m)	Pumping	[250 µm - 2 mm]	La Daana et al. (La Daana et al., 2017)

#### 4.3. Influence of the salt-wedge dynamics on microplastics dispersion

Observations and simulation results have shown that salt-wedge structure and river flow also impacts the flushing capacity and the abundance of microplastics. Observations revealed the presence of concentration peaks during the tidal cycles, which can be attributed to bottom particle resuspension and/or damping of turbulent mixing by density stratification at the arrival of the salt-wedge. Simulation results confirmed that turbulence damping by density stratification induces sinking of negatively buoyant microplastics, resulting in an accumulation at the bottom of the water column. Similar features were observed in the Ebro Estuary by Simon-Sánchez et al. (2019). In estuaries where the salt-wedge structure is quasi static, the salinity front acts as a barrier for dense plastic material transported as bed load (Acha et al., 2003). As the Adour estuary demonstrated a quasi-static salt-wedge structure at neap tide during dry season, we could expect similar mechanisms to take place under such conditions but with a total shift to another transport regime in different discharge and tide conditions (Defontaine et al., 2019). Therefore, the understanding and prediction of the salt-wedge dynamics is of major importance in the management of plastics pollution (Vermeiren et al., 2016) and merits further dedicated high-resolution studies. Microplastics dynamics is also driven by the riverine forcing. Observations of higher microplastics concentrations for higher river discharge are here only based on two contrasted cases. The observed trends need to be confirmed by more comprehensive sampling in wider ranges of conditions. However, these observations are in line with existing observations of a positive correlation between river discharge and abundance of microplastics (Lima et al., 2015; Lima et al., 2014; Rodrigues et al., 2019), associating the abundance increase with higher land and city drainage during flood events. Simulations showed that stronger river flow is also responsible for increased flushing capacity of the estuary. This is due to stronger ebbing currents and associated turbulence being able to transport more particles in suspension out of the estuary. Combining high discharge, higher contamination and enhanced flushing capacity, the strong flood events are then expected to be a major contributor to the contamination of coastal and oceanic waters, and should therefore be monitored accordingly.

#### 4.4. Simulation hypothesis and limitations

A series of numerical simulations have been performed to provide further insight on the microplastics dispersion processes in the Adour Estuary. Microplastics were treated as an Eulerian concentration field assuming that particle size and flow regime ensured that the particles closely follow the local flow. This approach remains consistent as long as the Stokes number of the particle, i.e. the ratio between the particle relaxation time scale to the local turbulence time scale, remains small and as long as the particle concentration remains small enough to neglect interactions between particles, which is generally the case for microplastics in open marine waters. Therefore the microplastics can be simulated as a passive tracer by solving an advection-diffusion equation for the concentration including a settling velocity, the only difference with natural sediment being lower density and settling velocity for most polymer particles. Several recent works support this approach by demonstrating significant correlation between microplastics and fine sediment (Rodrigues et al., 2019; Vianello et al., 2013). Both are affected by similar transport, sinking and accumulation mechanisms (Browne et al., 2010; Rodrigues et al., 2019). Microplastics may also be impacted by aggregation mechanisms similar to those affecting fine sediments, as a result of interaction with seawater and degradation mechanisms (Besseling et al., 2017; Long et al., 2015).

Note that, for the sake of simplicity, the turbulent diffusion for microplastics in the present numerical simulations was based on the assumptions of a turbulent Schmidt number equal to 1: microplastics and momentum are expected to diffuse at a similar rate, with a diffusion

coefficient computed by the turbulence model. The current knowledge of microplastics diffusion in a turbulent, and possibly stratified, flow field remains very limited. Recent high-resolution laboratory measurements suggested that microplastics turbulent Schmidt numbers can significantly differ from 1 (Poulain-Zarcos et al., 2020). Such research effort should be strongly fostered and extended to a wide range of real-world microplastics in order to improve the prediction performance of circulation models.

Numerical models are powerful tools and they usefully complement in-situ experimentations. To provide a better insight into the dynamics of microplastics contamination throughout the estuarine hydrosystem, simulations using more realistic configurations, including time-resolved river discharge for flood events, microplastic inputs at real sewage plant locations and/or diffuse runoff contamination will be performed. To that end, a major effort should be engaged to better monitor the microplastics inputs in the estuarine system, including incoming fluxes from each tributary, wastewater discharges and coastal waters contamination in wider ranges of conditions. It remains a considerable challenge given the difficulties of operating in such contexts. The role of particle properties such as shape, size, density, and settling velocity also deserves further examination. For more realistic simulations, properties of microplastics collected during the field campaign should be determined in the laboratory and considered in the simulations. Nevertheless, such properties are known to be variable and time-dependent under the action of biofouling, aggregation and fragmentation (Chubarenko et al., 2018; Vermeiren et al., 2016; Wright et al., 2013). In particular, understanding and predicting the effect of biofouling on microplastics dispersion in a time-dependent salt-wedge estuary remains a stiff challenge, as the growth and decay of biofilms and the related modifications of settling velocity are intrinsically linked to the light exposure, temperature and salinity conditions (Kooi et al., 2017) which all show strong variations at various time and space scales throughout the estuarine system. Constant settling velocity was a first step for the present study and more complex dynamic properties can be introduced in the model in a future study. In addition, it should be borne in mind that no wind effect was considered in the present simulations due to its a priori weaker influence on the inner estuary dynamics compared to tide and discharge, in relation with an overall weak wind forcing and short fetch in the considered section of the Adour Estuary. Wind stress at the free surface is expected to add turbulence mixing near the surface (Kukulka et al., 2012) and direct stress on floating particles (Forsberg et al., 2020). These effects will be explored in further studies once the specific roles played by the two main drivers, namely tide and discharge, have been well assessed.

As a final note, the present study leads us to emphasize the need for further research on the complementarity and the confrontation between field sampling and numerical modelling in microplastics dispersion. Field sampling is and will remain the central tool to estimate microplastics contamination. However, the cost of field sampling, both in terms of field operations and subsequent laboratory analysis, is so heavy that a comprehensive 3D time-resolved and long-term analysis of a complex and dynamic hydrosystem such as a salt-wedge estuary will remain out of reach using conventional sampling technologies. Field sampling should therefore be considered as providing snapshots of the local contamination, without any historical and spatial knowledge of microplastics dispersion. On the other hand, Eulerian numerical simulations are a powerful tool to provide insight on the spatial and temporal patterns of change in contamination and are therefore a useful complement to field sampling. The validity of the numerical results relies on the quality of the simulated hydrodynamics (Defontaine et al., 2018) and on the assumption that microplastics can be treated as an Eulerian concentration field, as discussed above. Direct comparisons between model results and field measurements would require total control of the initial and boundary conditions within the model, with a complete knowledge of the microplastics contamination levels and particle features at the initiation of the simulations and from each

potential microplastics input during the simulation. Further research work will be dedicated to this ambitious challenge, based on the fundamental knowledge gained with the present study.

## 5. Conclusion

The present study provided a first characterization of microplastics pollution in the Adour Estuary which is a major tributary of the southeastern Bay of Biscay. Field samplings confirmed, as for many other urban estuaries, persistent microplastic pollution. Mean abundance was estimated at 1.13 part/m<sup>3</sup>, with maximum values reaching 3.88 part/m<sup>3</sup> at the bottom of the water column. Microplastics were found from the surface to the near-bottom layer, emphasizing the need to sample the entire water column to estimate relevant contamination levels and fluxes. To focus only on the surface concentrations could lead to underestimation of pollution levels. Five types of microplastics were identified, in which films and fragments were the most abundant. The microplastics concentration was observed to be higher in high discharge conditions, leading to much higher total flux.

Numerical modelling showed that both local time-dependent and density-varying hydrodynamic conditions and microplastics properties have a determining influence on the particle dispersion, resulting in high spatial and temporal variability of abundance and distribution. The main trend was that neutrally-buoyant microplastics were easily flushed out while heavier particles were prone to be trapped in the estuary, in particular during low discharge conditions. The higher concentrations of microplastics as well as the higher proportion of fine microplastics found in the near bottom layer suggest that estuaries could be a sink of microplastics.

## CRediT authorship contribution statement

Sophie Defontaine: Methodology, Software, Validation, Formal analysis, Data curation, Investigation, Writing – Original draft Damien Sous: Conceptualization, Methodology, Investigation, Resources, Writing – Review and editing, Supervision, Project administration, Funding acquisition Javier Tesan: Investigation, Methodology Mathilde Monperrus: Investigation, Resources, Writing – Review and editing Véronique Lenoble: Methodology, Resources, Writing – Review and editing, Funding acquisition Laurent Lanceleur: Investigation, Writing – Review and editing.

## Declaration of competing interest

The authors declare that they have no known competing financial interests or personal relationships that could have appeared to influence the work reported in this paper.

## Acknowledgements

This study was sponsored by the MIDYNET project (EC2CO/CNRS) and the BIGCEES project (E2S UPPA). We are grateful to the port of Bayonne for the support with the sampling.

## References

- Abbas, S., Soltani, N., Keshavarzi, B., Moore, F., Turner, A., Hassanaghaei, M., 2018. Microplastics in different tissues of fish and prawn from the musa estuary, persian gulf. *Chemosphere* 205, 80–87.
- Acha, E.M., Mianzan, H.W., Iribarne, O., Gagliardini, D.A., Lasta, C., Daleo, P., 2003. The role of the ro de la plata bottom salinity front in accumulating debris. *Mar. Pollut. Bull.* 46 (2), 197–202.
- Alvim, C.B., Mendoza-Roca, J., Bes-Piá, A., 2020. Wastewater treatment plant as microplastics release source—quantification and identification techniques. *J. Environ. Manag.* 255, 109739.
- Andrady, A.L., 2011. Microplastics in the marine environment. *Mar. Pollut. Bull.* 62 (8), 1596–1605.
- Bakir, A., Rowland, S.J., Thompson, R.C., 2014. Transport of persistent organic pollutants

- by microplastics in estuarine conditions. *Estuar. Coast. Shelf Sci.* 140, 14–21.
- Barboza, L.G.A., Gimenez, B.C.G., 2015. Microplastics in the marine environment: current trends and future perspectives. *Mar. Pollut. Bull.* 97 (1–2), 5–12.
- Bellafont, F., Morichon, D., Roever, V., André, G., Abadie, S., 2018. Infragravity period oscillations in a channel harbor near a river mouth. *Coastal Engineering Proceedings* 1 (36), 8.
- Besseling, E., Quik, J.T., Sun, M., Koelmans, A.A., 2017. Fate of nano-and microplastic in freshwater systems: a modeling study. *Environ. Pollut.* 220, 540–548.
- Boucher, J., Friot, D., 2017. Primary Microplastics in the Oceans: A Global Evaluation of Sources. IUCN, Gland, Switzerland.
- Brennecke, D., Duarte, B., Paiva, F., Caçador, I., Canning-Clode, J., 2016. Microplastics as vector for heavy metal contamination from the marine environment. *Estuar. Coast. Shelf Sci.* 178, 189–195.
- Browne, M.A., Dissanayake, A., Galloway, T.S., Lowe, D.M., Thompson, R.C., 2008. Ingested microscopic plastic translocates to the circulatory system of the mussel, *Mytilus edulis* (L.). *Environ. Sci. Technol.* 42 (13), 5026–5031.
- Browne, M.A., Galloway, T.S., Thompson, R.C., 2010. Spatial patterns of plastic debris along estuarine shorelines. *Environ. Sci. Technol.* 44 (9), 3404–3409.
- Browne, M.A., Crump, P., Niven, S.J., Teuten, E., Tonkin, A., Galloway, T., Thompson, R., 2011. Accumulation of microplastic on shorelines worldwide: sources and sinks. *Environ. Sci. Technol.* 45 (21), 9175–9179.
- Burchard, H., Schuttelaars, H., Ralston, D., 2018. Sediment trapping in estuaries. *Annu. Rev. Mar. Sci.* 10, 371–395. <https://doi.org/10.1146/annurev-marine-010816-060535>.
- Cadiou, J.-F., Gerigny, O., Koren, Š., Zeri, C., Kaberi, H., Alomar, C., Panti, C., Fossi, M., Adamopoulou, A., Digka, N., et al., 2020. Lessons learned from an intercalibration exercise on the quantification and characterisation of microplastic particles in sediment and water samples. *Mar. Pollut. Bull.* 154, 111097.
- Chubarenko, I., Esiukova, E., Bagaev, A., Isachenko, I., Demchenko, N., Zobkov, M., Efimova, I., Bagaeva, M., Khatmullina, L., 2018. Behavior of microplastics in coastal zones. In: *Microplastic Contamination in Aquatic Environments*. Elsevier, pp. 175–223 Ch. 6.
- Collignon, A., Hecq, J.-H., Galgani, F., Collard, F., Goffart, A., 2014. Annual variation in neustonic micro-and meso-plastic particles and zooplankton in the Bay of Calvi (Mediterranean-Corsica). *Mar. Pollut. Bull.* 79 (1–2), 293–298.
- Covernton, G.A., Pearce, C.M., Gurney-Smith, H.J., Chastain, S.G., Ross, P.S., Dower, J.F., Dudas, S.E., 2019. Size and shape matter: a preliminary analysis of microplastic sampling technique in seawater studies with implications for ecological risk assessment. *Sci. Total Environ.* 667, 124–132.
- Crawford, C., Quinn, B., 2017. Microplastics, standardisation and spatial distribution. In: *Microplastic Pollutants*. Elsevier, pp. 101–130 Ch. 5.
- Cressey, D., 2016. Bottles, bags, ropes and toothbrushes: the struggle to track ocean plastics. *Nature News* 536 (7616), 263.
- Cutroneo, L., Reboa, A., Besio, G., Borgogno, F., Canesi, L., Canuto, S., Dara, M., Enrile, F., Forioso, I., Greco, G., et al., 2020. Microplastics in seawater: sampling strategies, laboratory methodologies, and identification techniques applied to port environment. *Environ. Sci. Pollut. Res.* 1–15.
- Declerck, A., Delpey, M., Rubio, A., Ferrer, L., Basurko, O., Mader, J., Louzao, M., 2019. Transport of floating marine litter in the coastal area of the south-eastern bay of Biscay: a Lagrangian approach using modelling and observations. *Journal of Operational Oceanography* 12 (sup2), S111–S125.
- Defontaine, S., 2019. Saline Structure, Circulation and Suspended Sediment Transport in a Channelized Salt-wedge Estuary: The Adour River Estuary. Ph.D. thesis. Université de Pau et des pays de l'Adour.
- Defontaine, S., Morichon, D., Sous, D., Monperrus, M., 2018. A combined numerical/experimental approach to understand stratification and mixing processes in the Adour estuary. In: *XVIIth International Symposium on Oceanography of the Bay of Biscay (ISOBAY 16)*, (Anglet, France).
- Defontaine, S., Sous, D., Morichon, D., Verney, R., Monperrus, M., 2019. Hydrodynamics and spm transport in an engineered tidal estuary: the Adour river (France). *Estuar. Coast. Shelf Sci.* 231, 106445.
- DiBenedetto, M.H., Ouellette, N.T., Koseff, J.R., 2018. Transport of anisotropic particles under waves. *J. Fluid Mech.* 837, 320–340.
- do Sul, J.A.I., Costa, M.F., 2014. The present and future of microplastic pollution in the marine environment. *Environ. Pollut.* 185, 352–364.
- Dris, R., Gasperi, J., Tassin, B., 2018. Sources and fate of microplastics in urban areas: A focus on Paris megacity. In: *Freshwater Microplastics*. Springer, Cham, pp. 69–83.
- Fok, L., Cheung, P.K., 2015. Hong Kong at the pearl river estuary: a hotspot of microplastic pollution. *Mar. Pollut. Bull.* 99 (1–2), 112–118.
- Forsberg, P., Sous, D., Stocchino, A., Chemi, R., 2020. Behaviour of plastic litter in nearshore waters: first insights from wind and wave laboratory experiments. *Mar. Pollut. Bull.* 153 (1–6).
- Gago, J., Henry, M., Galgani, F., 2015. First observation on neustonic plastics in waters off nw Spain (spring 2013 and 2014). *Mar. Environ. Res.* 111, 27–33.
- Galgani, F., Leaute, J., Moguedet, P., Souplet, A., Verin, Y., Carpentier, A., Goraguer, H., Latrouite, D., Andral, B., Cadiou, Y., et al., 2000. Litter on the sea floor along european coasts. *Mar. Pollut. Bull.* 40 (6), 516–527.
- Galgani, F., Fleet, D., Van Franeker, J., Katsanevakis, S., Maes, T., Mouat, J., Oosterbaan, L., Poitou, I., Hanke, G., Thompson, R., et al., 2010. Marine Strategy Framework Directive-Task Group 10 Report Marine Litter do Not Cause Harm to the Coastal and Marine Environment. Report on the Identification of Descriptors for the Good Environmental Status of European Seas Regarding Marine Litter Under the Marine Strategy Framework Directive. Office for Official Publications of the European Communities.
- Gallagher, A., Rees, A., Rowe, R., Stevens, J., Wright, P., 2016. Microplastics in the solent estuarine complex, UK: an initial assessment. *Mar. Pollut. Bull.* 102 (2), 243–249.
- Gray, A.D., Wertz, H., Leads, R.R., Weinstein, J.E., 2018. Microplastic in two South Carolina estuaries: occurrence, distribution, and composition. *Mar. Pollut. Bull.* 128, 223–233.
- Hervouet, J.-M., 2007. *Hydrodynamics of Free Surface Flows: Modelling With the Finite Element Method*. vol. 360 Wiley Online Library.
- Hidalgo-Ruz, V., Gutow, L., Thompson, R.C., Thiel, M., 2012. Microplastics in the marine environment: a review of the methods used for identification and quantification. *Environ. Sci. Technol.* 46 (6), 3060–3075.
- Isobe, A., Kako, S., Chang, P.-H., Matsuno, T., 2009. Two-way particle-tracking model for specifying sources of drifting objects: application to the East China Sea shelf. *J. Atmos. Ocean. Technol.* 26 (8), 1672–1682.
- Jalón-Rojas, I., Wang, X.-H., Fredj, E., 2019. On the importance of a three-dimensional approach for modelling the transport of neustic microplastics. *Ocean Sci.* 15 (3), 717–724.
- Kako, S., Isobe, A., Seino, S., Kojima, A., 2010. Inverse estimation of drifting-object outflows using actual observation data. *J. Oceanogr.* 66 (2), 291–297.
- Khatmullina, L., Isachenko, I., 2017. Settling velocity of microplastic particles of regular shapes. *Mar. Pollut. Bull.* 114 (2), 871–880.
- Kooi, M., Nes, E.H.v., Scheffer, M., Koelmans, A.A., 2017. Ups and downs in the ocean: effects of biofouling on vertical transport of microplastics. *Environ. Sci. Technol.* 51 (14), 7963–7971.
- Kowalski, N., Reichardt, A.M., Wanek, J.J., 2016. Sinking rates of microplastics and potential implications of their alteration by physical, biological, and chemical factors. *Mar. Pollut. Bull.* 109 (1), 310–319.
- Kukulka, T., Proskurowski, G., Morét-Ferguson, S., Meyer, D., Law, K., 2012. The effect of wind mixing on the vertical distribution of buoyant plastic debris. *Geophys. Res. Lett.* 39 (7).
- La Daana, K.K., Officer, R., Lyshevskaya, O., Thompson, R.C., O'Connor, I., 2017. Microplastic abundance, distribution and composition along a latitudinal gradient in the Atlantic Ocean. *Mar. Pollut. Bull.* 115 (1–2), 307–314.
- Law, K.L., 2017. Plastics in the marine environment. *Annu. Rev. Mar. Sci.* 9, 205–229.
- Lebreton, L.C., Van Der Zwet, J., Damsteeg, J.-W., Slat, B., Andradý, A., Reisser, J., 2017. River plastic emissions to the world's oceans. *Nat. Commun.* 8, 15611.
- Lebreton, L.-M., Greer, S., Borroto, J.C., 2012. Numerical modelling of floating debris in the world's oceans. *Mar. Pollut. Bull.* 64 (3), 653–661.
- Lenz, R., Enders, K., Stedmon, C.A., Mackenzie, D.M., Nielsen, T.G., 2015. A critical assessment of visual identification of marine microplastic using raman spectroscopy for analysis improvement. *Mar. Pollut. Bull.* 100 (1), 82–91.
- Li, H.-X., Ma, L.-S., Lin, L., Ni, Z.-X., Xu, X.-R., Shi, H.-H., Yan, Y., Zheng, G.-M., Rittschof, D., 2018. Microplastics in oysters *saccostrea cucullata* along the pearl river estuary, China. *Environ. Pollut.* 236, 619–625.
- Lima, A., Costa, M., Barletta, M., 2014. Distribution patterns of microplastics within the plankton of a tropical estuary. *Environ. Res.* 132, 146–155.
- Lima, A., Barletta, M., Costa, M., 2015. Seasonal distribution and interactions between plankton and microplastics in a tropical estuary. *Estuar. Coast. Shelf Sci.* 165, 213–225.
- Long, M., Moriceau, B., Gallinari, M., Lambert, C., Huvet, A., Raffray, J., Soudant, P., 2015. Interactions between microplastics and phytoplankton aggregates: impact on their respective fates. *Mar. Chem.* 175, 39–46.
- Lusher, A.L., Burke, A., O'Connor, I., Officer, R., 2014. Microplastic pollution in the Northeast Atlantic Ocean: validated and opportunistic sampling. *Mar. Pollut. Bull.* 88 (1–2), 325–333.
- Mani, T., Hauk, A., Walter, U., Burkhardt-Holm, P., 2015. Microplastics profile along the Rhine river. *Sci. Rep.* 5 (1), 1–7.
- Masiá, P., Ardura, A., García-Vazquez, E., 2019. Microplastics in special protected areas for migratory birds in the bay of Biscay. *Mar. Pollut. Bull.* 146, 993–1001.
- Mccormick, A.R., Hoellein, T.J., London, M.G., Hittie, J., Scott, J.W., Kelly, J.J., 2016. Microplastic in surface waters of urban rivers: concentration, sources, and associated bacterial assemblages. *Ecosphere* 7 (11), e01556.
- Mendoza, A., Osa, J.L., Basurko, O.C., Rubio, A., Santos, M., Gago, J., Galgani, F., Peña-Rodriguez, C., 2020. Microplastics in the bay of Biscay: an overview. *Mar. Pollut. Bull.* 153, 110996.
- Murray, C.C., Maximenko, N., Lippia, S., 2018. The influx of marine debris from the great Japan tsunami of 2011 to North American shorelines. *Mar. Pollut. Bull.* 132, 26–32.
- Naidoo, T., Glassom, D., Smit, A.J., 2015. Plastic pollution in five urban estuaries of Kwazulu-Natal, South Africa. *Mar. Pollut. Bull.* 101 (1), 473–480.
- Neumann, D., Callies, U., Matthies, M., 2014. Marine litter ensemble transport simulations in the southern north sea. *Mar. Pollut. Bull.* 86 (1–2), 219–228.
- Peng, G., Zhu, B., Yang, D., Su, L., Shi, H., Li, D., 2017. Microplastics in sediments of the changjiang estuary, China. *Environ. Pollut.* 225, 283–290.
- Poulain-Zarcos, M., ter Halle, A., Mercier, M., 2020. Vertical distribution of particles in upper-ocean turbulence: Laboratory modelling of plastic pollution. In: *Ocean Sciences Meeting 2020*. AGU.
- Rezania, S., Park, J., Din, M.F.M., Taib, S.M., Talaiekhozani, A., Yadav, K.K., Kamyab, H., 2018. Microplastics pollution in different aquatic environments and biota: a review of recent studies. *Mar. Pollut. Bull.* 133, 191–208.
- Rodrigues, S., Almeida, C.M.R., Silva, D., Cunha, J., Antunes, C., Freitas, V., Ramos, S., 2019. Microplastic contamination in an urban estuary: abundance and distribution of microplastics and fish larvae in the douro estuary. *Sci. Total Environ.* 659, 1071–1081.
- Sadri, S.S., Thompson, R.C., 2014. On the quantity and composition of floating plastic debris entering and leaving the tamar estuary, Southwest England. *Mar. Pollut. Bull.* 81 (1), 55–60.
- Sherman, P., Van Sebille, E., 2016. Modeling marine surface microplastic transport to assess optimal removal locations. *Environ. Res. Lett.* 11 (1), 014006.

- Simon-Sánchez, L., Grelaud, M., García-Orellana, J., Ziveri, P., 2019. River deltas as hotspots of microplastic accumulation: the case study of the Ebro river (NW Mediterranean). *Sci. Total Environ.* 687, 1186–1196.
- Sous, D., Defontaine, S., Morichon, D., Bhairy, N., Lanceleur, L., Monperrus, M., 2018. Turbulence measurements in a stratified man-controlled estuary, the adour case. In: XVIth International Symposium on Oceanography of the Bay of Biscay (ISOBAY 16), (Anglet, France).
- Stocchino, A., De Leo, F., Besio, G., 2019. Sea waves transport of inertial micro-plastics: mathematical model and applications. *Journal of Marine Science and Engineering* 7 (12), 467.
- Sutton, R., Mason, S.A., Stanek, S.K., Willis-Norton, E., Wren, I.F., Box, C., 2016. Microplastic contamination in the San Francisco bay, California, USA. *Mar. Pollut. Bull.* 109 (1), 230–235.
- Thompson, R.C., Olsen, Y., Mitchell, R.P., Davis, A., Rowland, S.J., John, A.W., McGonigle, D., Russell, A.E., 2004. Lost at sea: where is all the plastic? *Science* 304 (5672), 838.
- van Sebille, E., England, M.H., Froyland, G., 2012. Origin, dynamics and evolution of ocean garbage patches from observed surface drifters. *Environ. Res. Lett.* 7 (4), 044040.
- Vermeiren, P., Muñoz, C.C., Ikejima, K., 2016. Sources and sinks of plastic debris in estuaries: a conceptual model integrating biological, physical and chemical distribution mechanisms. *Mar. Pollut. Bull.* 113 (1–2), 7–16.
- Vianello, A., Boldrin, A., Guerriero, P., Moschino, V., Rella, R., Sturaro, A., Da Ros, L., 2013. Microplastic particles in sediments of lagoon of Venice, Italy: first observations on occurrence, spatial patterns and identification. *Estuar. Coast. Shelf Sci.* 130, 54–61.
- Willis, K.A., Eriksen, R., Wilcox, C., Hardesty, B.D., 2017. Microplastic distribution at different sediment depths in an urban estuary. *Front. Mar. Sci.* 4, 419.
- Wright, S.L., Thompson, R.C., Galloway, T.S., 2013. The physical impacts of microplastics on marine organisms: a review. *Environ. Pollut.* 178, 483–492.
- Xanthos, D., Walker, T.R., 2017. International policies to reduce plastic marine pollution from single-use plastics (plastic bags and microbeads): a review. *Mar. Pollut. Bull.* 118 (1–2), 17–26.
- Xu, P., Peng, G., Su, L., Gao, Y., Gao, L., Li, D., 2018. Microplastic risk assessment in surface waters: a case study in the Changjiang estuary, China. *Mar. Pollut. Bull.* 133, 647–654.
- Yan, M., Nie, H., Xu, K., He, Y., Hu, Y., Huang, Y., Wang, J., 2019. Microplastic abundance, distribution and composition in the pearl river along Guangzhou city and pearl river estuary, China. *Chemosphere* 217, 879–886.
- Yonkos, L.T., Friedel, E.A., Perez-Reyes, A.C., Ghosal, S., Arthur, C.D., 2014. Microplastics in four estuarine rivers in the Chesapeake bay, USA. *Environ. Sci. Technol.* 48 (24), 14195–14202.
- Zhao, S., Zhu, L., Wang, T., Li, D., 2014. Suspended microplastics in the surface water of the Yangtze estuary system, China: first observations on occurrence, distribution. *Mar. Pollut. Bull.* 86 (1–2), 562–568.
- Zhao, S., Zhu, L., Li, D., 2015. Microplastic in three urban estuaries, China. *Environ. Pollut.* 206, 597–604.